JOURNAL OF GEOPHYSICAL RESEARCH, VOL. 99, NO. D7, PAGES 14,481–14,491, JULY 20, 1994

Analysis of cloud top height and cloud coverage from satellites using the O_2 *A* and *B* bands

Akihiko Kuze and Kelly V. Chance
Harvard-Smithsonian Center for Astrophysics, Cambridge, Massachusetts

Abstract. Cloud height and cloud coverage detection are important for total ozone retrieval using ultraviolet and visible scattered light. Use of the O_2 *A* and *B* bands, around 761 and 687 nm, by a satellite-borne instrument of moderately high spectral resolution viewing in the nadir makes it possible to detect cloud top height and related parameters, including fractional coverage. The measured values of a satellite-borne spectrometer are convolutions of the instrument slit function and the atmospheric transmittance between cloud top and satellite. Studies here determine the optical depth between a satellite orbit and the Earth or cloud top height to high accuracy using FASCODE 3. Cloud top height and a cloud coverage parameter are determined by least squares fitting to calculated radiance ratios in the oxygen bands. A grid search method is used to search the parameter space of cloud top height and the coverage parameter to minimize an appropriate sum of squares of deviations. For this search, nonlinearity of the atmospheric transmittance (i.e., leverage based on varying amounts of saturation in the absorption spectrum) is important for distinguishing between cloud top height and fractional coverage. Using the above-mentioned method, an operational cloud detection algorithm which uses minimal computation time can be implemented.

1. Introduction

More than 50% of the Earth's surface is covered with clouds. Cloud height and cloud coverage detection are important for a number of atmospheric measurement purposes, including total ozone retrieval and distinction between the stratospheric and tropospheric O_3 burdens using ultraviolet and visible scattered light. The Nimbus 7 total ozone mapping spectrometer and solar backscattered ultraviolet instruments use scattered solar ultraviolet light for ozone profile and total ozone retrieval [*Fleig et al.*, 1990]. They estimate cloud coverage from measured reflectivity at 340 nm, assuming that the cloud top exists uniformly at a pressure of 0.4 atm. For improvement in environmental monitoring, more detailed cloud detection is required.

To collect enough photons for the required signal-to-noise ratios in measurements, a spaceborne spectrometer usually has a larger instantaneous field of view (IFOV) than radiometers like the thematic mapper (LandSat-D) and Système Probatoire d'Observation de la Terre. The large IFOV of the spectrometer will often include both cloud-containing and cloud-free areas. High spatial resolution cloud distribution data are obtained by the spaceborne radiometers, but it is difficult for them to detect cloud height.

Figure 1 shows the calculated radiance in the O_2 visible region for complete coverage in a few cloud type cases using the radiative transfer model MODTRAN [*Berk et al.*, 1989] in the case of $\theta = 60°$ and $\varphi = 0°$, where θ is the solar zenith angle and φ is the nadir-viewing angle. The absolute level of the measured radiance depends on the cloud type. Also, it is difficult to distinguish cloud from Earth albedo variation. Thus a method providing direct information on the atmospheric structure, such as the measurement of relative radiances using absorption lines, is necessary for improved cloud parameter detection. Use of the O_2 *A* and *B* bands, around 761 and 687 nm, is such a method, one which we will demonstrate makes it possible to detect cloud height and coverage parameters simultaneously from a nadir-viewing instrument. Cloud altitude estimation using the O_2 *A* band was suggested by *Yamamoto and Wark* [1961], and a detailed study was done by *Wark and Mercer* [1965]. *Saiedy et al.* [1967] determined cloud top height on a Gemini mission using a spacecraft-borne spectrograph camera with 0.5-nm resolution. *Fisher and Grassl* [1991] and *Fisher et al.* [1991] measured the O_2 *A* band with an airborne 0.6-nm spectral resolution spectrometer having high spatial resolution and detected cloud top height with 50-m accuracy. However, it is rare that an entire IFOV for a satellite-based spectrometer (typically 100 × 100 km) is covered evenly by a cloud layer. Therefore cloud coverage detection is also important. We show that using a moderately high (approximately 4.0-cm^{-1} resolution) spectrometer and measuring in several absorption channels, both cloud top height and cloud coverage detection become possible.

The study done here is a prototype for the Global Ozone Monitoring Experiment (GOME) and the scanning imaging absorption spectrometer for atmospheric chartography (SCIAMACHY), which are European satellite instruments designed primarily for atmospheric trace gas measurements. GOME and SCIAMACHY are both diode array-based spectrometers, which measure the atmospheric spectrum with continuous coverage from 240 to 790 nm at a resolution of about 0.1 nm in the ultraviolet and 0.2 nm in the visible. Measurements in this region are expected to provide determinations of the atmospheric trace species O_3, NO_2, and BrO, and the more abundant species O_2, $(O_2)_2$, and H_2O, and have prospects for measuring H_2CO, SO_2, ClO, and

Paper number 94JD01152.
0148-0227/94/94JD-01152$05.00

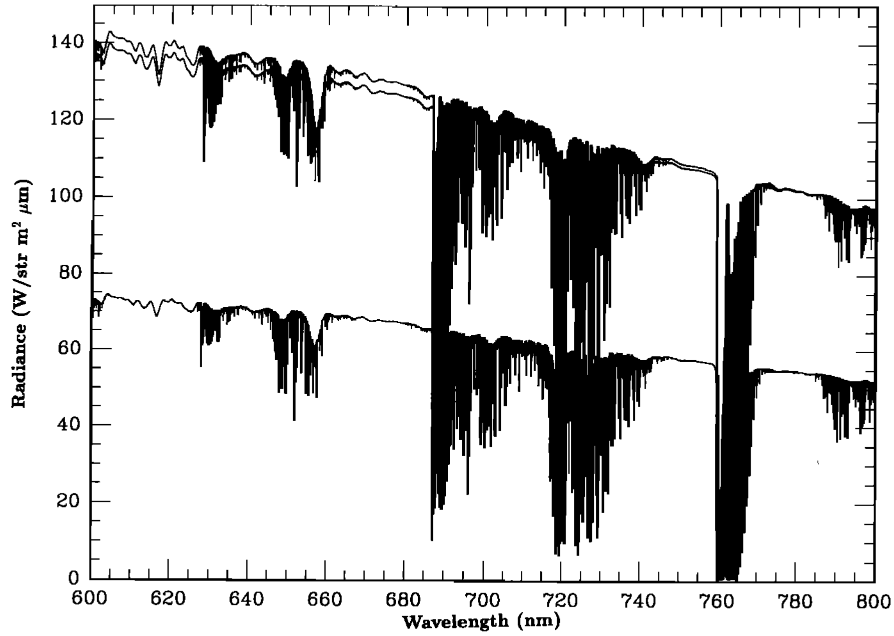

Figure 1. Calculated radiance in the visible region, including the O_2 *A* and *B* bands, for complete coverage of selected cloud types. From the top, altostratus, stratus, and cloud free.

OClO under special conditions. The wavelength coverage of both instruments includes the ultraviolet Hartley and Huggins bands and the visible Chappuis bands of O_3. The continuous spectral coverage of SCIAMACHY continues into the infrared, to 1700 nm, with additional detector arrays at 2.0 and 2.3 μm. GOME is a nadir-viewing instrument, while SCIAMACHY includes a nadir-viewing mode. Both have the capability to make measurements at the resolution and accuracy needed for application of the principles investigated in the present study. GOME is scheduled for launch on the European Space Agency's ERS 2 satellite in late 1994/early 1995, while SCIAMACHY will be a part of the Envisat 1 payload in the late 1990s. The simultaneous detection of cloud parameters will help considerably in trace gas retrievals for these instruments. For ozone in particular, the concentration peaks in the stratosphere (nominally at ~23 km), well above normal cloud altitudes. However, ozone in the troposphere makes a nonnegligible contribution to the total column density, one which may be growing as a result of anthropogenic activities. A major impetus for this study is the correction of ozone measurements in order to permit both better statistical evaluation of global ozone column measurements and determination of the climatology of tropospheric ozone.

In the ultraviolet and visible regions, incident light at different wavelengths penetrates to almost the same distance inside of clouds; the effective cloud top height does not depend strongly on wavelength. Thus measurements of the O_2 *A* and *B* bands are useful for 300- to 400-nm cloud top height detection, appropriate to measurements in Hartley and Huggins bands of O_3, as well as in the visible Chappuis bands. Both GOME and SCIAMACHY will be capable of detecting both cloud top height and cloud coverage with moderate accuracy when combined with appropriate atmospheric modeling capability. The remainder of this paper will discuss the cloud detection capability specifically in terms of GOME, but the discussion is equally applicable to SCIAMACHY nadir-viewing measurements.

In this study we calculate the dependence of the measured spectrum on the cloud top height and a cloud coverage parameter (specifically, the product of the fractional coverage times the cloud reflectivity, αr, divided by the scene-averaged albedo, γ) for several cases of instrument resolution, wavelength coverage, and cloud conditions. A minimization technique is applied in order to determine the range of values which correspond most closely to the measurement. The scene-averaged albedo can be determined independently by measurements out of the O_2 bands in order to determine αr. Complete determination of the fractional coverage currently depends on independent knowledge of either the cloud reflectivity or the ground albedo. In future work we hope to be able to demonstrate techniques for simultaneous retrieval of cloud reflectivity and ground albedo as well as cloud top height and cloud coverage with instruments of sufficient resolution and sensitivity. Such retrieval would remove the ambiguity in the coverage parameter and its dependence on climatological values of cloud top reflectivity and Earth albedo.

2. Radiative Transfer in the O_2 Absorption Region

Figure 2 shows the O_2 *A* and *B* spectral bands, calculated using the 1992 HITRAN database [*Rothman et al.*, 1992]. O_2 *A* and *B* have strong absorption around 13,143 cm^{-1} (761 nm) and 14,546 cm^{-1} (687 nm). (Note that wavelength, in nanometers, is the unit of choice for measurements by the satellite instruments, which are dispersive spectrometers. Line parameter listings are normally in cm^{-1}, since line shapes are appropriately described in a scale linear in energy.) A spectrometer with a spectral resolution of about 4.0 cm^{-1} (e.g., GOME) will have several spectral measure-

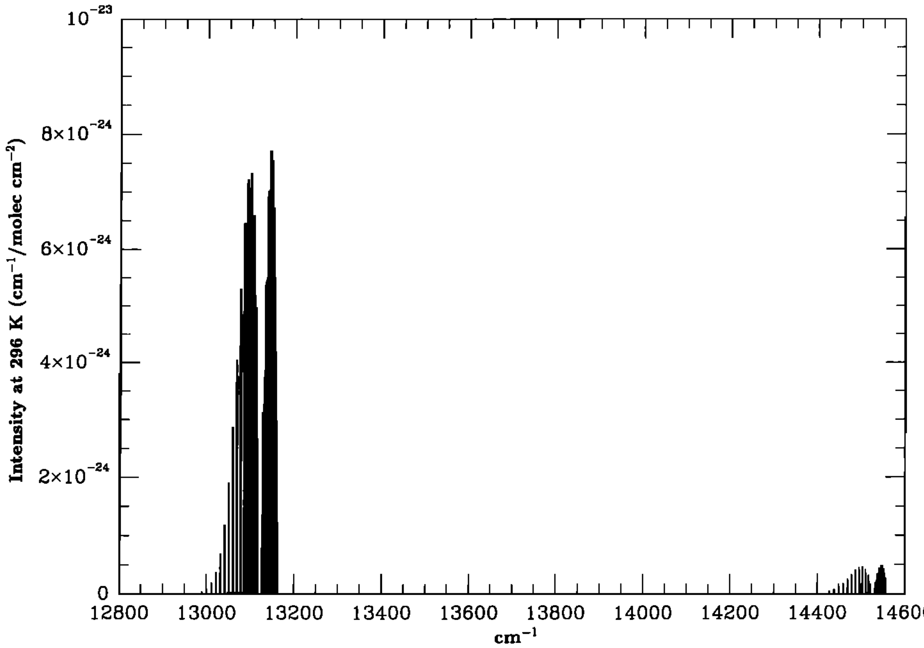

Figure 2. A stick spectrum showing the O_2 *A* and *B* band positions and intensities from the 1992 HITRAN database.

ments in the O_2 bands. The radiance measured in the satellite geometry by spectral channel j, neglecting scattering, is described by

$$I(j) = \sum_{i=1}^{N} \alpha_{ij} r_i \int f_j(\nu) F(\nu) \exp\left(-s\tau(\nu, h_i)\right) \frac{d\nu}{\Delta\nu}$$

$$+ \beta_j \left(1 - \sum_{i=1}^{N} r_i\right) \int f_j(\nu) F(\nu) \exp\left(-s\tau(\nu, 0)\right) \frac{d\nu}{\Delta\nu}, \qquad (1)$$

where N is the number of different cloud top height types, α_{ij} is the cloud top reflectivity for cloud type i in spectral channel j, r_i is the coverage of type i cloud, $f_j(\nu)$ is the slit function of channel j, $F(\nu)$ is the solar spectrum, $\tau(\nu, h)$ is the optical depth between cloud top and satellite (proportional to total O_2 column amount above the cloud top), h_i is the top height of type i cloud, $\Delta\nu$ is the full spectral width at half maximum of the instrument, and β_j is the Earth's surface diffusive albedo. Here α_{ij} and β_j are assumed to be constant over the small spectral size of spectrometer channel considered here. The optical path factor s is $\sec(\theta) + \sec(\varphi)$. The cloud type definitions that we use correspond to those of LOWTRAN and MODTRAN [*Kneizys et al.*, 1988; *Berk et al.*, 1989]. The major effect of different cloud types (except for cirrus, as noted below) is to change the radiance level of the reflected radiation. From studies such as the MODTRAN calculations shown in Figure 1, we can assume that clouds are thick enough that solar light reflects at the cloud tops; this is the operational definition of "cloud top" in these studies. There are several caveats in this assumption. If a cloud layer is not sufficiently thick that determination of a cloud top height to the ~1-km accuracy aimed for in this study is possible, there will obviously be an ambiguity in the determination. Different cloud types may have bidirectional reflectance distribution functions (BRDFs) that differ sufficiently that the reflectance calculations at different viewing and solar zenith angles are significantly affected; this aspect of the problem is currently under investigation at the University of Bremen, Bremen, Germany, (J. Burrows, R. Spurr, and T. Kurosu, private communication, 1993). The effect of cirrus clouds on the determination of cloud parameters deserves, and will get, more attention than it has received in this study. Our current feeling is that optically thin cirrus will not present a significant problem; clouds that are partially transmitting have the same effect when averaged over the instrumental field of view as a partial coverage. Multiple Mie scattering inside of clouds may significantly affect the optical path; the size of this effect is currently being investigated at the University of Heidelberg, Heidelberg, Germany, with Monte Carlo multiple scattering calculations (H. Frank and U. Platt, private communication, 1993). This specifically includes an investigation into potential multiple scattering problems in cirrus. The effect of multiple scattering inside clouds may be the limiting factor in the general applicability of optical methods in cloud determinations. Radiance in the absence of absorption by O_2 or other gases (e.g., out of band), without scattering, is described as

$$I_0(j) = \gamma_j \int F(\nu) f_j(\nu) \frac{d\nu}{\Delta\nu}, \qquad (2)$$

where

$$\gamma_j = \sum_{i=1}^{N} \alpha_{ij} r_i + \beta_j \left(1 - \sum_{i=1}^{N} r_i\right).$$

For GOME, $F(\nu)$ is determined from a priori information and on-board solar flux monitoring using a diffuser. Thus the scene-averaged albedo γ_j out of band can be directly determined.

Scattering effects are considered below. In the above wavelength region, absorptions by gases other than O_2 are small compared with the dominant O_2 absorption; they can be safely neglected for cloud detection at the present level of accuracy. In the O_2 A and B bands, γ_j is interpolated using the spectrum near the O_2 A and B bands where there is no strong absorption. The slit function $f_j(\nu)$ is assumed to be triangular, because the spaceborne spectrometers we are considering have the same output slit (detector) size as the entrance slit. In the real measurements the slit function must, of course, be measured with high spectral resolution. The vertical profiles of O_2 number density and temperature are assumed to be well known. Optical depths $\tau(\nu, h)$ between the satellite orbit and each height are calculated with high accuracy using FASCODE 3 (G. P. Anderson and J. H. Chetwynd, private communication, 1992).

The measured values are convolutions of the slit function, $I_0(\nu)$, and the atmospheric transmittance. By analogy with *Fleig et al.* [1990] it is convenient to describe the convolution in terms of a parameter Q, defined in our case as

$$Q(j, h_i) = \int f_j(\nu) \exp(-s\tau(\nu, h_i)) \frac{d\nu}{\Delta\nu}. \quad (3)$$

The parameter $R(\nu_0, h_i)$, which is the ratio of satellite-measured radiation to solar input radiation, is then defined by the following, assuming $F(\nu)$ is constant within a spectrometer channel so that it can be taken outside of the integral in equations (1) and (2):

$$R(j, h_i, \alpha_{ij}r_i) = \frac{I(j)}{F(\nu)}$$

$$= \sum_{i=1}^{N} \alpha_{ij}r_iQ(j, h_i) + \beta_j(1 - \sum_{i=1}^{N} r_i)Q(j, 0)$$

$$= \sum_{i=1}^{N} \alpha_{ij}r_iQ(j, h_i) + (\gamma_j - \sum_{i^\circ 1}^{N} \alpha_{ij}r_i)Q(j, 0) \quad (4)$$

3. Determination of Cloud Top Height and Related Parameters

3.1. Grid Search Least Squares Fit

Cloud parameters are determined by least squares fitting to calculated radiance ratios. We assume there is no a priori information on h_i and $\alpha_{ij}r_i$ in equation (4) and use a grid search method to search the parameter space of h_i, $\alpha_{ij}r_i$ to minimize the variance. The quantity χ^2 is defined as

$$\chi^2 = \sum_{j=1}^{M} \left(\frac{R_{\text{obs}}(j, h_i, \alpha_{ij}r_i) - R_{\text{calc}}(j, h_i, \alpha_{ij}r_i)}{R_{\text{obs}}(j, h_i, \alpha_{ij}r_i)} \right)^2 \bigg/ M, \quad (5)$$

where the R_{obs} are R values from measurement and dividing by the measured solar calibration, the R_{calc} are R values for grid searching to determine h_i and α_ir_i, and M is the number of spectrometer channels in the O_2 A and B band regions (α_{ij} and γ_j are assumed to be constant within each O_2 band).

Here χ^2 is not divided by the error value σ^2, because σ^2 is almost the same for each spectrometer channel. The σ^2 attained in the measurements determines the contour describing the level of accuracy achieved in cloud parameters, as shown below. The ranges of r_i and h_i are between 0 and 1 and between 0 and 10 km, respectively. In the present work, grid searching is used rather than a continuous nonlinear least squares technique, since we are evaluating χ^2 over a space of variables with discrete values. No particular attempt has yet been made to optimize the technique; rather, we perform complete evaluations of χ^2 over the range of coverage variable at ~0.01 resolution and over cloud-top height at ~0.1-km resolution. Because the ranges and resolutions are limited, the computation time necessary to search the resulting tables for minimum values is not a serious concern.

For both cloud top height and cloud coverage detection, optical depth is an important concern. If the optical thickness is too large, it becomes impossible to detect low cloud accurately, because the Q values become too small. If the optical depth is too small, the transmittance is an almost linear function of α_ir_i and optical depth, and it becomes impossible to distinguish cloud height from cloud coverage. If the difference of integrated optical depth between channels is too small, it is also impossible to distinguish cloud height from cloud coverage. Thus for cloud parameter detection, both the optical depth values and contrast between channels are important.

Figures 3a and 3b show calculated optical depths for a range of typical cloud top height scenarios using FASCODE 3: Figure 3a for the O_2 A band and Figure 3b for the O_2 B band. Around this spectral region the GOME resolution is about 4.0 cm^{-1}. The optical depths change substantially in this region, so calculations must be done with high spectral resolution. When the spectral resolution is much wider than the oxygen spectral lines in the bands, the measured optical depth is a highly averaged or smeared-out quantity and its variation with detector channel is small. Therefore higher spectral resolution improves cloud detection. Figure 4 shows Q values for several A and B band channels in the case of $\Delta\nu$ = 4.0 cm^{-1} and s = 2.0. The center positions of the channels are 13,132, 13,144, 14,539, and 14,551 cm^{-1}.

We have calculated the variation of χ^2 in the space of cloud top height versus the coverage parameter α_1r_1/γ for representative cases of instrumental resolution, number of measuring channels, and cloud top heights. The results are given in Figure 5 as contour plots showing the logarithm of χ^2; these plots are intended to give a visual sense of how well a minimization scheme (such as the grid search employed here) will succeed in the independent determination of cloud top height and the coverage parameter. Figure 5a shows the variation of χ^2 for a typical GOME case, $\Delta\nu$ = 4.0 cm^{-1}, N = 1, and M = 12, with a cloud layer at 5 km and a coverage parameter of α_1r_1/γ = 0.5 (50% coverage when the cloud top reflectivity is equal to the Earth albedo). The twelve spectrometer channels chosen consist of seven O_2 A and five O_2 B band measurements. The center positions of the channels are 13,132, 13,136, 13,140, . . . 13,156 cm^{-1} for the O_2 A band and 14,539, 14,543, 14,547, . . . 14,555 cm^{-1} for the O_2 B band. N = 1 is assumed because there will most often be one cloud type within the IFOV. Figure 5b compares this case with that of higher spectral resolution, $\Delta\nu$ = 0.2 cm^{-1}. The center positions of the channels are 13,150.6, 13,150.8, 13,151.0, . . . 13,151.8 cm^{-1} for the O_2 A band and

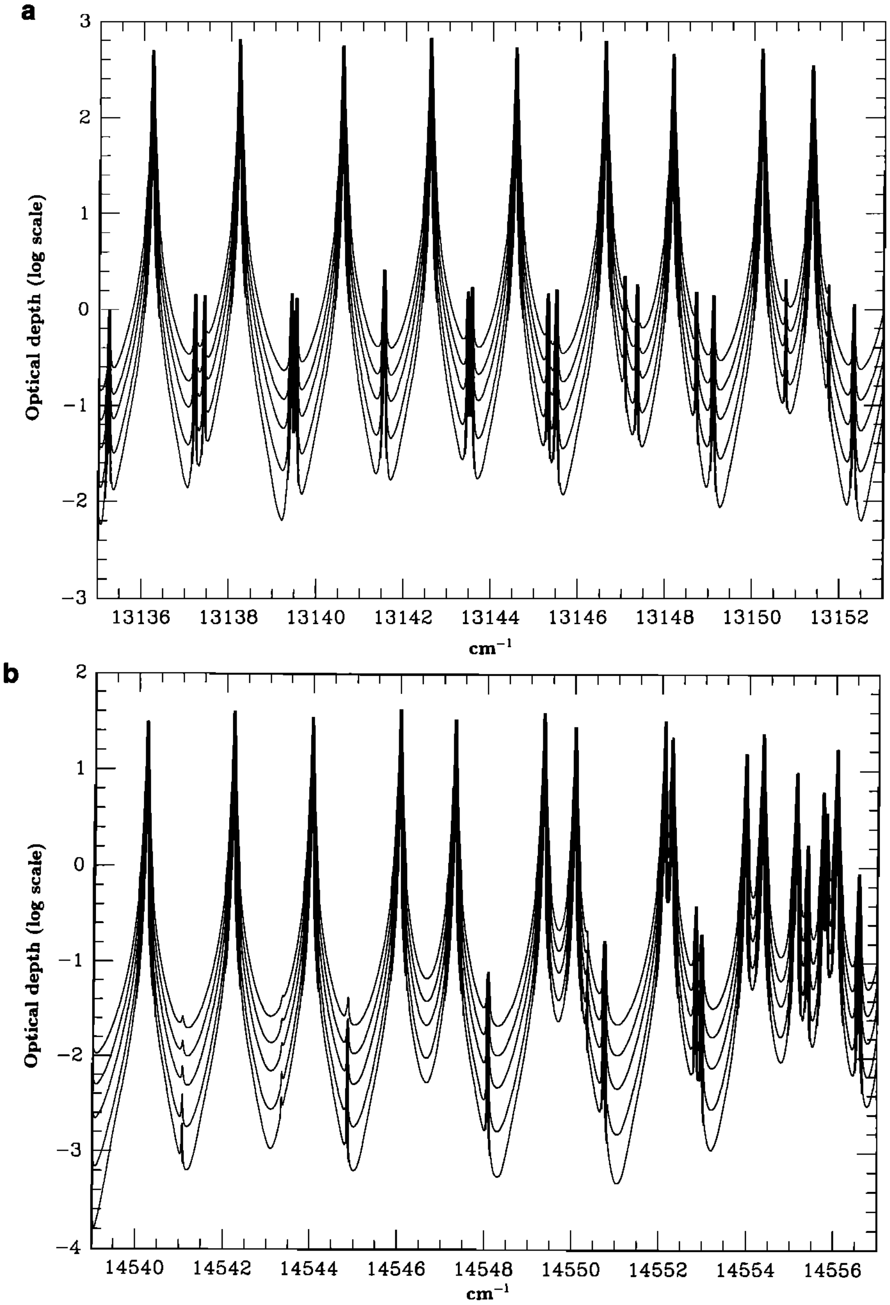

Figure 3. Calculated nadir optical depths for the visible bands of O_2 between space and the altitudes 0 (top), 2, 4, 6, and 8 (bottom) km: (a) O_2 *A* band and (b) O_2 *B* band.

14,555.1, 14,555.3, 14,555.5, ... 14,555.9 cm^{-1} for the O_2 *B* band. Figures 5c and 5d show cases of a lower cloud top height (2 km) with $\Delta\nu = 4.0$ cm^{-1} and $\Delta\nu = 0.20$ cm^{-1} as in Figures 5a and 5b. Figure 5c has several minima, but the proper one is significantly deeper; if the measurement accuracy is very good, the solution is unique. For the lower-altitude cloud and lower spectral resolution there are extended trough regions in the variation of χ^2 with cloud height versus cloud coverage. This indicates that high accuracy is required in order to get a unique solution for cloud coverage. Generally, higher resolution is better for cloud detection, but there may be a tradeoff here between resolution and signal-to-noise ratio. However, as Figure 5c shows, cloud height is easily determined. For total ozone retrieval, the coverage of low cloud may not be critically important. From the hyperbolic shapes of the contours in Figure 5c we may conclude that for low cloud top height and low cloud coverage, the cloud top height is not accurately determined. On the other hand, for the higher cloud top height and higher coverage case, both height and coverage detection accuracy is high. There is a basic tradeoff in cloud coverage versus cloud height information that stems from the fact that the most basic accurate information obtained by measurements in the O_2 bands, which is that of absorption in the optically thin portions of the bands, gives the average transmission or, equivalently, path length through the atmosphere. Any overestimate of cloud coverage thus implies an underestimate in cloud top height. Figures 5e and 5f are moderate- and

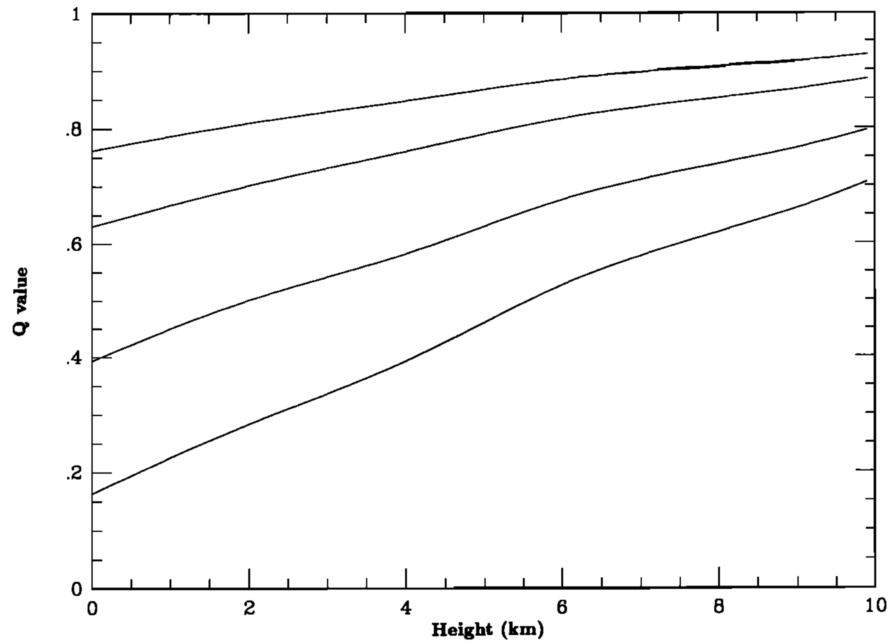

Figure 4. Q values (convolutions of the instrument slit function and the atmospheric transmittance) for O_2 A and B band channels with center positions of 14,539, 14,551, 13,132, and 13,144 cm^{-1} (top to bottom) for instrument resolution $\Delta\nu = 4.0$ cm^{-1}.

high-resolution cases of $M = 2$, $r_1 = 0.5$, and $h_1 = 5$ km. These are calculated in order to compare results obtained with differing numbers of measurement channels. The resolution is 4.0 cm^{-1}, and the center wavelengths of the channels are 13,140 and 14,547 cm^{-1} for Figure 5e; the resolution is 0.2 cm^{-1}, and the center wavelengths of the channels are 13,151.0 and 14,555.5 cm^{-1} for Figure 5f. Comparison of Figures 5e and 5a shows clearly that the use of a large number of spectral channels greatly improves the accuracy for moderate (i.e., GOME) resolution. However, for higher spectral resolution, a small number of spectral channels is adequate, as shown by Figure 5f.

The above method determines $\alpha_1 r_1$. By using interpolated values of γ_j, $\beta(1 - r_1)$ may also be determined. If appropriate a priori data for β are available, α_1 and r_1 may be determined individually. From the α_1 value it may be possible to estimate the cloud depth. This study is for one cloud type and cloud top height, but the determination of two or more cloud layers within the IFOV may be possible with the use of a grid search in more than four dimensions.

3.2. Accuracy Requirements and Error Estimation

The desired uniqueness of solution determines the accuracy requirement. As mentioned above, for lower-height cloud detection, high accuracy is required. This statement can be quantified in a typical example. Figure 6 indicates the $|\chi|$ variation for $N = 1$, $M = 12$, $r_1 = 0.5$, $h_1 = 5$ km, and $\Delta\nu = 4.0$ cm^{-1}. As before, the twelve spectrometer channels include seven in the A band and five in the B band. The central contour, shown as a bold line, corresponds to the limit of ±1% measurement error about the central minimum. This contour corresponds to ±20% error in cloud coverage and ±2 km in cloud top height. If the cloud coverage detection accuracy is required to be ±20%, the sum of measurement error and model calculation error must be less than 1%. The anticipated random errors in measurements are small enough to allow precise solution (the modeled signal-to-noise ratio for GOME is ~1000), but the forward model calculations in the present study have uncertainties which may cause substantial systematic error. It is possible to detect the area surrounded by the contour line in Figure 6 when the systematic errors are 1%. This area indicates the correlation between cloud top and cloud coverage and should be useful for removing cloud effects in total ozone determinations. To separate cloud top height and coverage accurately, higher spectral resolution is required. The significant systematic error sources are discussed below. These items are expected to be corrected by adequate calibration.

Measurement errors. Because R is a ratio, that of the Earth measurement to the solar measurement, the systematic radiance errors of the instrument response largely cancel. The capability for relative radiance measurements should be better than 1%.

Model calculation errors include the items listed below. The first two items affect both γ and Q value calculations. The third affects γ, and the others affect the Q values.

Single and multiple scattering effects. As discussed below, scattering effects must be included for accurate cloud determination.

Effects of other gases. There are strong H_2O bands between the O_2 A and B bands, but they do not affect the O_2 A and B bands significantly. In FASCODE 3 studies we find the calculated optical depth due to other gases within the O_2 A and B band limits to be negligible.

Scene-averaged albedo interpolation in the O_2 A and B bands. The solar spectrum can be assumed to decrease linearly around the O_2 A and B bands. The error caused by interpolation is negligibly small.

Line parameter database. As discussed below, the line

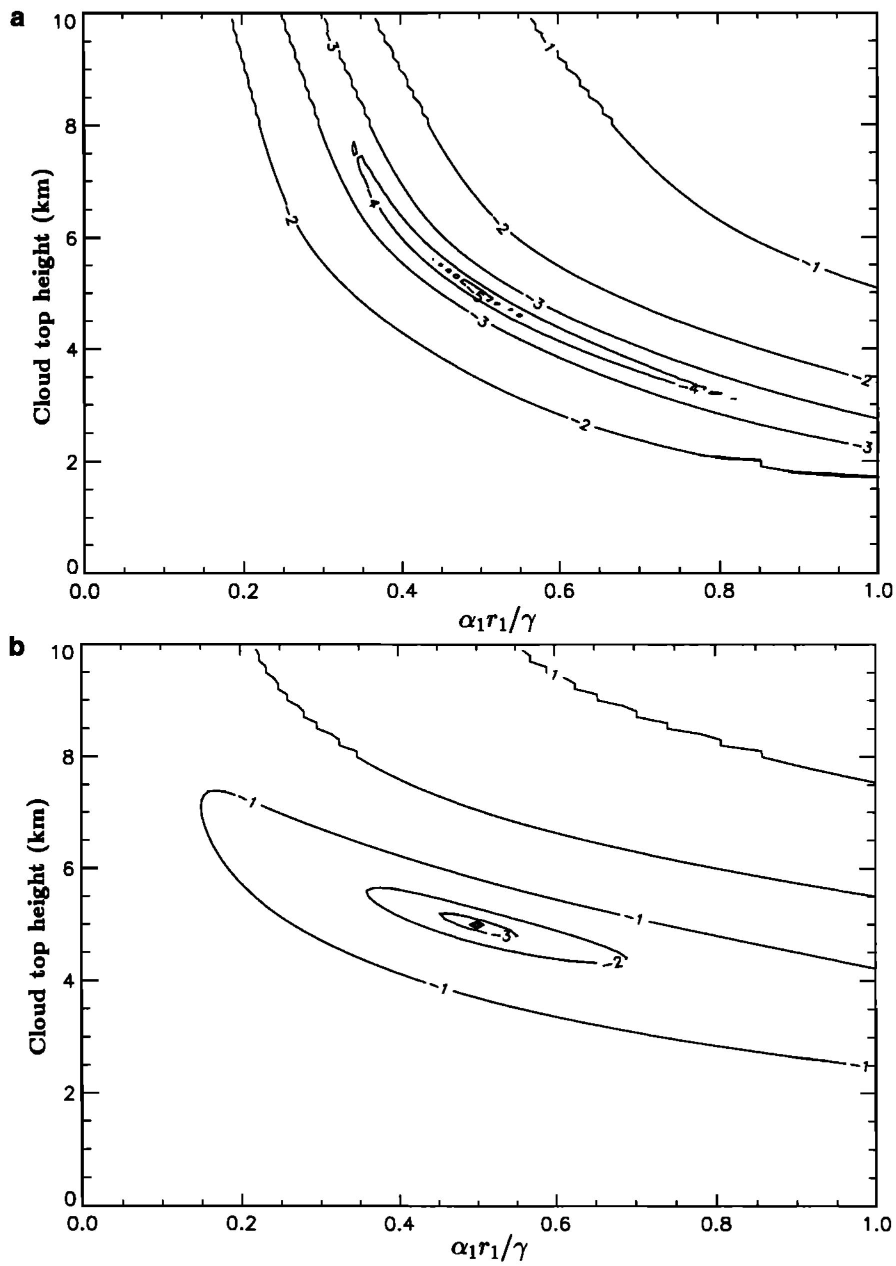

Figure 5. The χ^2 variation in log scale, where χ^2 is the sum of squares of radiance ratio deviations, which is minimized in the fitting process to determine cloud-top height and coverage (see text for details). Estimated uncertainties are not included in χ^2; rather, the uncertainties determine which contour is applicable. Results are presented for several case studies illustrating differences due to the number of measurement channels, M; the height of the cloud layer, h; and the instrument resolution, $\Delta\nu$. The cloud coverage parameter, $\alpha_1 r_1/\gamma = 0.5$, includes a ratio of albedos, as explained in the text. (a) $M = 12$, $\alpha_1 r_1/\gamma = 0.5$, $h = 5$ km, and $\Delta\nu = 4.0$ cm^{-1}; (b) $M = 12$, $\alpha_1 r_1/\gamma = 0.5$, $h = 5$ km, and $\Delta\nu = 0.2$ cm^{-1}; (c) $M = 12$, $\alpha_1 r_1/\gamma = 0.5$, $h = 2$ km, and $\Delta\nu = 4.0$ cm^{-1}; (d) $M = 12$, $\alpha_1 r_1/\gamma = 0.5$, $h = 2$ km, and $\Delta\nu = 0.2$ cm^{-1}; (e) $M = 2$, $\alpha_1 r_1/\gamma = 0.5$, $h = 5$ km, and $\Delta\nu = 4.0$ cm^{-1}; and (f) $M = 2$, $\alpha_1 r_1/\gamma = 0.5$, $h = 5$ km, and $\Delta\nu = 0.2$ cm^{-1}.

intensities and pressure-broadening coefficients must be determined to high accuracy compared to that of the desired detection accuracy, or an appropriate in-flight characterization and calibration scheme must be used.

Temperature profiles. According to the *Wark and Mercer* [1965] absorptance calculations, the effect of temperature profile ambiguity on optical depth calculations in these bands (at low spectral resolution) is less than 1%. A calculational check of the temperature dependences for selected individual line strengths confirms this conclusion for the stronger lines in the *A* band.

Slit function. The absolute value of spectral responsivity is not a concern in this method. The shape of the modeled instrument slit function is, however, extremely important.

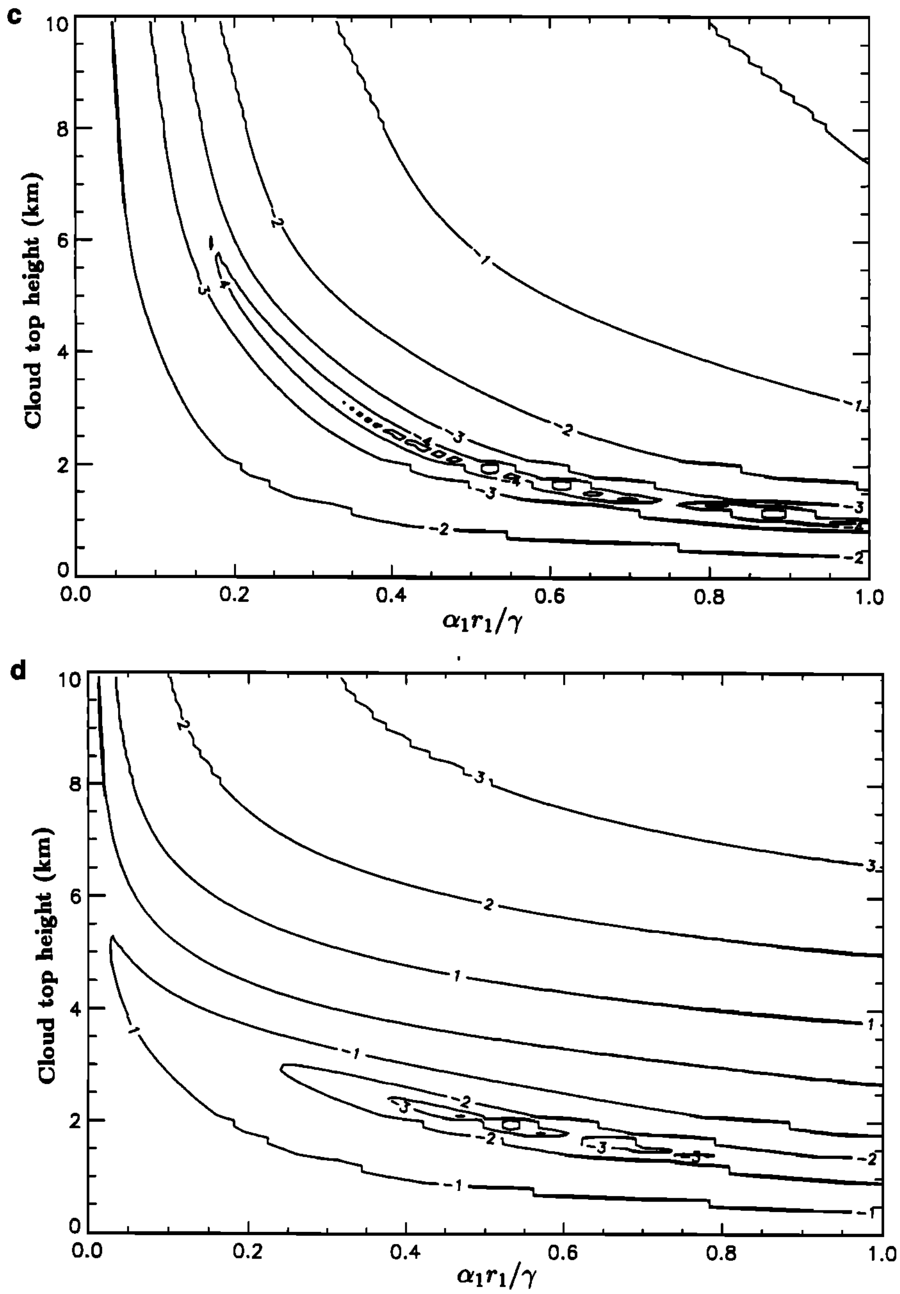

Figure 5. (continued)

Extra absorption inside clouds. The estimated cloud top is always below the actual cloud top because of the extra absorption inside the clouds [cf. *Saiedy et al.*, 1967]. For our present purposes of correcting for ozone and other trace species, the important consideration is whether multiple Mie scattering within the cloud, of light that is eventually scattered back out into the instrument field of view, is a severe limitation. If the major effect of penetration into the cloud is replacement of the cloud top by a diffuse scattering surface at a lower altitude, then the technique is perfectly suited for such correction. This problem is not thought to be serious at the present (1 km) level of accuracy, but the previously mentioned calculations underway at the Universities of Bremen and Heidelberg will provide more definitive answers to this concern.

3.3. Algorithm and Operation

Before launch, the optical depths necessary to determine Q values are calculated for several temperature profile scenarios at a resolution of 0.001 cm^{-1}, and the slit function is measured at similarly high resolution. Look-up tables in terms of optical depth are then prepared at intervals of ~0.1 km.

After launch, the operational software searches for the minimum χ^2 and estimates the cloud top heights and coverage. The increments for heights and coverages are ~0.1 km and 1%, respectively. The default number of different cloud types within the IFOV, N, is 1. Thermal differences between ground calibration and orbit, including thermal cycling of the instrument through the satellite orbit, may cause the center wavelengths for the measurement channels to change. Thus

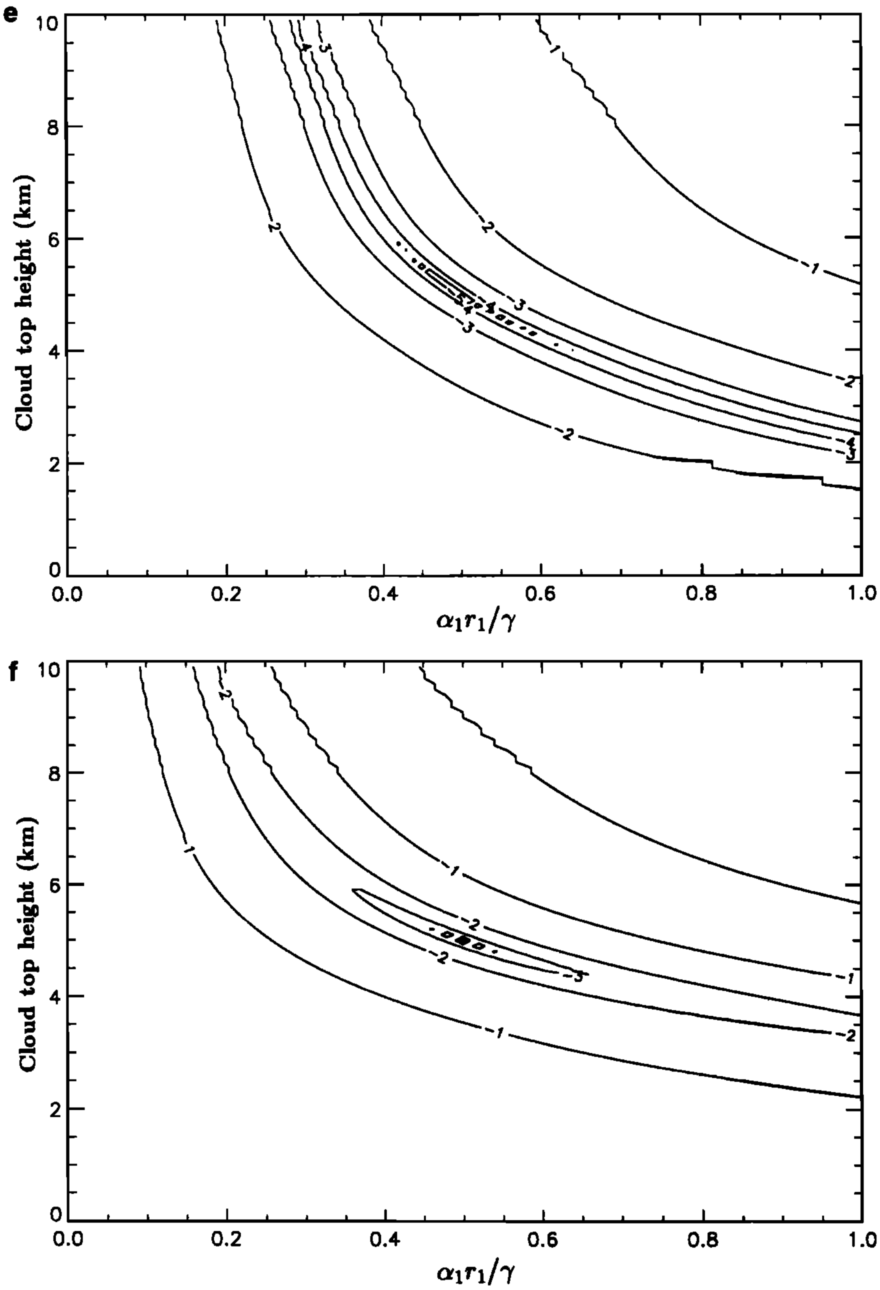

Figure 5. (continued)

Q values must be recalculated after the on-board wavelength calibration.

4. Discussion

4.1. Cloud Reflectivity and Earth Surface Albedo

Both $\alpha_1 r_1$ and $\beta(1 - r_1)$ are determined in this method. As mentioned above, in order to estimate cloud coverage and cloud reflectivity we will, as our initial working algorithm, employ an a priori Earth surface albedo table which includes both geographical and seasonal information. The source of the albedo database used to create this table is the ETOPO5 data set (NOAA/National Geophysical Data Center, Boulder, Colorado). More sophisticated future versions of the algorithm should exploit the radiance data from the satellite instrument itself further. GOME and SCIAMACHY each measure the scene-averaged albedo, γ_j, from 240 nm to 790 nm, including measurements in wide spectral regions where atmospheric gas absorptions are small. As β has substantially stronger wavelength dependence than α_1, this scene-averaged albedo information should help to further separate surface albedo and cloud coverage. Additionally, cloud scattering studies currently underway at the University of Bremen should provide invaluable information on cloud top reflection coefficients coupled to cloud type and altitude (J. Burrows, R. Spurr, and T. Kurosu, private communication, 1993). Thus we anticipate that the proper combination of the satellite radiance measurements and cloud scattering studies will provide the necessary leverage to separate albedo, cloud reflectivity, and coverage to high accuracy.

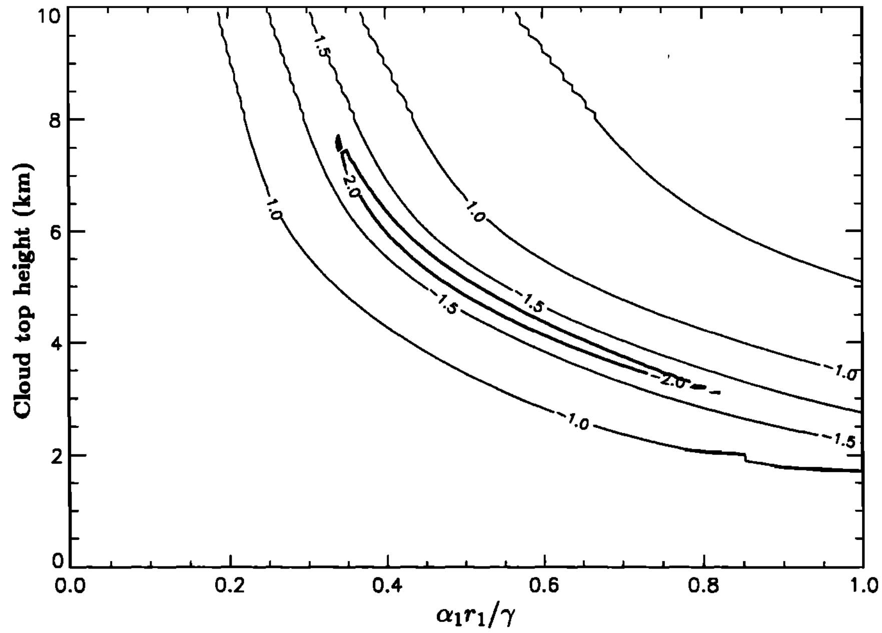

Figure 6. The $|\chi|$ variation in log scale; $M = 12$, $\alpha_1 r_1/\gamma = 0.5$, $h = 5$ km, and $\Delta\nu = 4.0$ cm^{-1}.

4.2. Scattering Effects

Even though Rayleigh scattering is small in the visible O_2 absorption region compared with the ultraviolet region covered by GOME, its effect in the atmospheric path must be considered for accurate cloud detection. Single-scattering radiance calculations do not depend on either the cloud top reflectivity or Earth surface albedo, but when multiple scattering is included, there is a strong dependence on both. Therefore to estimate scattering effects, a priori data of α and β are necessary. The input radiance $I_s(j)$, including scattering effects is

$$I_s(j) = r_1 \int f_j(\nu)(\alpha_1 F(\nu)T(s,\ \nu,\ h_1) + S(\nu,\ h_1,\ \alpha_1))\,\frac{d\nu}{\Delta\nu}$$
$$+ (1 - r_1) \int f_j(\nu)(\beta F(\nu)T(s,\ \nu,\ 0) + S(\nu,\ 0,\ \beta))\,\frac{d\nu}{\Delta\nu}, \tag{6}$$

where $T(s,\ \nu,\ h_1)$ is the transmittance and $S(\nu,\ h_1,\ x)$ is the single and multiple scattered radiance.

In general, reflectivity of cloud tops is high in the visible region. Therefore scattering effects are relatively small and radiance calculation errors are small. Out of the O_2 absorption region the scattering affects γ_j estimation. The difference between the radiance not considering scattering, $I_0(j)$, and the radiance considering scattering, $I_s(j)$, is less than 1% when $\beta = 0.3$, because the back-scattering ratio to the zenith is almost equal to the Earth surface diffusive reflectivity (note that geometry must be carefully considered when evaluating the importance of Rayleigh scattering in non-GOME geometries, though). A 10% ambiguity of a priori β in the $S(\nu,\ 0,\ \beta(\nu))$ calculation causes an error of a few percent in $I_s(j)$. Therefore the γ_j error caused by scattering is less than a few percent.

In the O_2 absorption region, scattering affects Q value calculations. Because the optical path, including the O_2 column density, is multiplied by scattering, the effective optical depth calculation depends on α and β. For low β, scattering effects on Q value estimation are relatively high. Therefore ambiguity in β might cause a serious error, and a priori data on β are important for estimation of scattering effects.

4.3. Spectral Band Database

The line parameters for these bands necessary to perform the quantitative analysis proposed here are included in the HITRAN and GEISA databases, derived from measurements by *Miller et al.* [1969] and *Giver et al.* [1974]. The line positions are well known for both bands. The intensities for the O_2 *B* band are well known (to better than 2%), but for the O_2 *A* band they are known to only 4%. For both bands, considerable work is necessary on line-broadening parameters. Pressure broadening is the chief determinant of line widths and thus of radiative transfer through the bands below about 8 km in the Earth's atmosphere.

O_2 broadening of the O_2 *A* band lines at room temperature is known to about 15%. No N_2 or air broadening studies have been made, and no temperature dependencies have been measured. The values used in the catalogs for O_2 *A* band broadening are actually the more accurately determined O_2 *B* band width parameters (see below), a substitution made on the presumption that the vibrational dependence of pressure-broadening coefficients is negligible. Studies for the magnetic dipole-allowed microwave rotationless and far infrared rotational lines [*Chance et al.*, 1991] show that (1) air broadening can be substantially different from O_2 broadening, (2) temperature dependence can differ substantially from the suggested hard sphere value of $T^{-0.5}$, and (3) state-to-state dependence, even when sharing a common lower state, can vary substantially between the microwave rotationless and far infrared rotational lines. This fact, plus experience with rotational and vibrational comparisons for other molecules, suggests that the O_2 *A* and *B* band broadening parameters may differ at a level that is important for detailed geophysical studies. The cumulative error in the widths under atmospheric conditions, considering all of these factors, may well exceed 25%.

The O_2 *B* band widths are in somewhat better shape, as they were performed at a later time using more fully developed techniques, but there are still only widths (albeit good to 2–3%) for room temperature O_2 broadening. Broadening values for this band also need to be expanded to include air broadening and low temperatures to be useful for realistic geophysical analysis.

Q value calculations depend directly on line intensities; 2% error in the intensities corresponds to a few percent error in *Q* value calculation. Although GOME and SCIAMACHY have a $\sim$4.0-cm^{-1} resolution, wider than the O_2 *A* and *B* band line widths, the *Q* values are sensitive to pressure broadening line widths both because the pressure broadening affects line saturation except in the optically thin limit and because the slit function is triangular and the *Q* values are proportional to convolutions of the line shape and the slit function. The exact sensitivity depends on the line center location in each channel. A 3% error in line width generally corresponds to less than a few percent error in *Q* value calculation.

Detailed sensitivity analyses to assess the precise effect of line parameter uncertainties on the cloud parameter retrieval accuracy are planned for the next phase of this investigation. This will include more detailed dependence of *Q* values on line parameters and on the measurement channel placement with respect to the peaks of the O_2 lines. Simple radiative transfer considerations imply that the determination of the scene average path length is a process that depends primarily on the optically thin components of the observations. We expect that at the first level of approximation, the knowledge of this quantity depends linearly upon the knowledge of the line intensities. We also expect that in order to be able to overcome potentially large systematic effects due to uncertainties in line parameters, an in-flight characterization and calibration scheme will need to be devised in order to effectively utilize any data other than optically thin absorption measurements.

5. Conclusions

GOME and SCIAMACHY have several channels of varying, but moderate, optical depth in the O_2 *A* and *B* band regions. We have proposed an operational method for determination of cloud parameters that has the potential to produce accurate results with minimal computation time. This method has been primarily developed as a contribution to the development of the GOME and SCIAMACHY programs. It has the potential to be effective for other satellite-based measurement programs as well, including geostationary meteorological satellite observations that employ larger IFOVs and longer integration times compared with the Sun synchronous satellite observations of GOME and SCIAMACHY. For accurate detection, further studies of spectral band parameters, scattering effects, and Earth albedo studies are required. Scattering studies currently underway include those of cloud-top reflection coefficients (BRDFs) coupled to cloud type and altitude (J. Burrows, R. Spurr, and T. Kurosu, private communication, 1993) and the Monte Carlo multiple scattering calculations of scattering inside clouds (H. Frank and U. Platt, private communication, 1993).

Acknowledgments. This research was supported by NASA grant NAGW-2541.

References

Berk, A., L. S. Bernstein, and D. C. Robertson, MODTRAN: A moderate resolution model for LOWTRAN 7, *AFGL Tech. Rep., 89-0122*, 1–42, 1989.

Chance, K. V., W. A. Traub, K. W. Jucks, and D. G. Johnson, On the use of O_2 spin-rotation lines for elevation angle calibration of atmospheric thermal emission spectra, *Int. J. Infrared Millimeter Waves, 12*, 581–588, 1991.

Fisher, J., and H. Grassl, Detection of cloud-top height from backscattered radiances within the oxygen A band, 1, Theoretical study, *J. Appl. Meteorol., 30*, 1245–1259, 1991.

Fisher, J., W. Cordes, A. Schmitz-Peiffer, W. Renger, and P. Mörl, Detection of cloud-top height from backscattered radiances within the oxygen A band, 2, Measurements, *J. Appl. Meteorol., 30*, 1260–1267, 1991.

Fleig, A. J., R. D. McPeters, P. K. Bhartia, B. M. Schlesinger, R. P. Cebula, K. F. Klenk, and D. F. Heath, Nimbus 7 solar backscatter ultraviolet (SBUV) ozone products user's guide, *NASA Ref. Publ., 1234*, 1–128, 1990.

Giver, L. P., R. W. Boese, and J. H. Miller, Intensity measurements, self-broadening coefficients, and rotational intensity distribution for lines of the oxygen B band at 6880 Å, *J. Quant. Spectrosc. Radiat. Transfer, 14*, 793–802, 1974.

Kneizys, F. X., E. P. Shettle, L. W. Abreu, J. H. Chetwynd, G. P. Anderson, W. O. Gallery, J. E. A. Selby, and S. A. Clough, Users guide to LOWTRAN 7, *AFGL Tech. Rep., 88-0177*, 1–137, 1988.

Miller, J. H., R. W. Boese, and L. P. Giver, Intensity measurements and rotational intensity distribution for the oxygen A band, *J. Quant. Spectrosc. Radiat. Transfer, 9*, 1507–1517, 1969.

Rothman, L. S., et al., The HITRAN molecular database editions of 1991 and 1992, *J. Quant. Spectrosc. Radiat. Transfer, 14*, 469–507, 1992.

Saiedy, F., H. Jacobowitz, and D. Q. Wark, On cloud-top determination from Gemini-5, *J. Atmos. Sci., 24*, 63–69, 1967.

Wark, D. G., and D. M. Mercer, Absorption in the atmosphere by the oxygen "A" band, *Appl. Opt., 4*, 839–844, 1965.

Yamamoto, G., and D. Q. Wark, Discussion of the letter by R. A. Hanel, "Determination of cloud altitude from a satellite," *J. Geophys. Res., 66*, 3596, 1961.

A. Kuze and K. V. Chance, Harvard-Smithsonian Center for Astrophysics, 60 Garden Street, Cambridge, MA 02138.

(Received June 1, 1993; revised March 24, 1994; accepted April 20, 1994.)